[PS]Connectivity of Pore Space: The Primary Control on Two-Phase Flow Properties of Tight-Gas Sands*

Maryam A. Mousavi[1] and Steven L. Bryant[2]

Search and Discovery Article #50222 (2009)
Posted November 20, 2009

*Adapted from poster presentation at AAPG Annual Convention and Exhibition, Denver, Colorado, June 7-10, 2009

[1]Petroleum Engineering, University of Texas at Austin, Austin, TX (mousavi@mail.utexas.edu)
[2]Petroleum Engineering, University of Texas at Austin, Austin, TX

Abstract

We use quantitative grain-scale models to predict the variation of capillary pressure curves in tight gas sandstones. We model several depositional and diagenetic processes important for porosity and permeability reduction in tight gas sands, such as having various amounts of ductile grains and quartz cementation. The model is purely geometric and begins by applying a cooperative rearrangement algorithm to produce dense, random packings of spheres of different sizes. We simulate the evolution of this model sediment into a low-porosity sandstone by applying different amount of ductile grains and quartz precipitation. To account for deformation of ductile (lithic) grains, we used the soft-shell model, in which grains can interpenetrate until their inner rigid cores come into contact. We varied the fraction of grains assumed to be ductile and the radius of the rigid core of the ductile grains. The overgrowth or rim cement was modeled by uniformly increasing the radius of all the grains, while holding their centers fixed. In this way we produce model tight sandstones having porosities between 3% and 10%. A substantial fraction (tens of percent) of the original pore throats in the sediment are closed by the simulated diagenetic alteration. It is known that overgrowth cement causes the pore space to drop below the percolation threshold when half of the throats are closed. Thus the pore space in typical tight gas sandstones is poorly connected, and is often close to being completely disconnected.

The drainage curve for different model rocks was computed using invasion percolation in a network taken directly from the grain-scale geometry and topology of the model. Some general trends follow classical expectations and are confirmed by experimental measurements: increasing the amount of cement or decreasing the rigid radius of ductile grains while holding other parameters constant shift the drainage curve to larger pressures. Adding more cement or reducing the rigid radius of ductile grains causes the irreducible water saturations to increase. However, simulation of different packings show significant variability in drainage curves even for model rocks with similar porosities and similar pore throat size distributions. The variability is large enough to mask the

general trends described above. We conclude that the connectivity of the matrix pore space is the most important factor for understanding flow properties of tight gas sandstones.

References

Haines, W.B., 1930, Studies in the Physical Properties of Soil, V. The Hysteresis Effects in Capillary Properties and the Modes of Moisture Distribution Associated Therewith, Journal of Agricultural Sciences, v. 20, p. 97.

Mason, G. and D.W. Mellor, 1995, Stimulation of drainage and imbibitions in a random packing of equal spheres: Journal of Colloid and Interface Science, v. 176, p. 214-225.

Mousavi, M.A. and S.L. Bryant, 2007, Geometric models of porosity reduction mechanisms in tight gas sands: Paper presented at Rocky Mountain Oil & Gas Technology Symposium, Denver, Colorado, April 2007.

AAPG Annual Convention & Exhibition 7-10 June 2009 Denver, Colorado

Connectivity of Pore Space: The Primary Control on Two-Phase Flow Properties of Tight-Gas Sands, AAPG 535743 (Part I)

Maryam A. Mousavi & Steven L. Bryant

Center for Petroleum and Geosystems Engineering, The University of Texas at Austin

Abstract

We use quantitative grain-scale models to predict the variation of capillary pressure curves in tight gas sandstones. We model several depositional and diagenetic processes important for porosity and permeability reduction in tight gas sands, such as having various amounts of ductile grains and quartz cementation. The model is purely geometric and begins by applying a cooperative rearrangement algorithm to produce dense, random packings of spheres of different sizes. We simulate the evolution of this model sediment into a low-porosity sandstone by applying different amount of ductile grains and quartz precipitation. To account for deformation of ductile (lithic) grains, we used the soft-shell model, in which grains can interpenetrate until their inner rigid cores come into contact. We varied the fraction of grains assumed to be ductile and the radius of the rigid core of the ductile grains. The overgrowth or rim cement was modeled by uniformly increasing the radius of all the grains, while holding their centers fixed. In this way we produce model tight sandstones having porosities between 3% and 10%. A substantial fraction (tens of percent) of the original pore throats in the sediment are closed by the simulated diagenetic alteration. It is known that overgrowth cement causes the pore space to drop below the percolation threshold when half of the throats are closed. Thus the pore space in typical tight gas sandstones is poorly connected, and is often close to being completely disconnected.

The drainage curve for different model rocks was computed using invasion percolation in a network taken directly from the grain-scale geometry and topology of the model. Some general trends follow classical expectations and are confirmed by experimental measurements: increasing the amount of cement or decreasing the rigid radius of ductile grains while holding other parameters constant shift the drainage curve to larger pressures. Adding more cement or reducing the rigid radius of ductile grains causes the irreducible water saturations to increase. However, simulation of different packings show significant variability in drainage curves even for model rocks with similar porosities and similar pore throat size distributions. The variability is large enough to mask the general trends described above. We conclude that the connectivity of the matrix pore space is the most important factor for understanding flow properties of tight gas sandstones.

Hypothesis

Simulations of drainage in model tight gas sandstones show significant variability even for model rocks with similar porosities and similar pore throat size distributions. We propose that this variability is intrinsic to tight gas sandstones because the pore space is so poorly connected.

Grain Scale Modeling

Cooperative Rearrangement Algorithm

1. Initial point generation
2. Growing the spheres
3. Overlap removal

Result: dense, disordered packing that represents sediment

Ductile Grain Simulation

1. Assignment of ductile characteristics to subset of grains,
2. Cooperative rearrangement of the mixture of rigid and ductile spheres
3. Volume conservation

Result: model rock in which porosity reduced by grain deformation

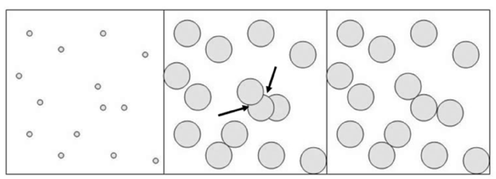

Fig. 1(a). The three steps of cooperative rearrangement algorithm. (left) Generation of initial sphere locations. (middle) Growth of spheres causing overlap (arrows). (right) Displacement of spheres to eliminate overlaps. The growth and displacement steps are iterated until no further growth is possible.

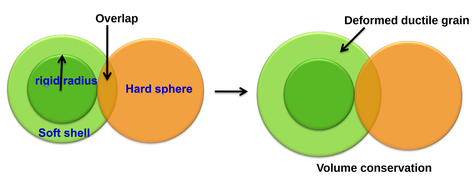

Fig. 1(b). In the volume conservation step, the amount of overlap between grains is calculated and added to the outer shell of ductile grain. Therefore the ductile grains become deformed, partial spheres.

Modeling of Ductile Grains

Fig. 2(a). Ductile deformation of mica-rich lithic; Penn. Breathitt Sandstone, South Appalachian Basin *(Image courtesy of Kitty Milliken, BEG)*

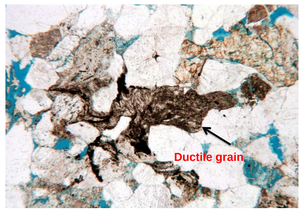

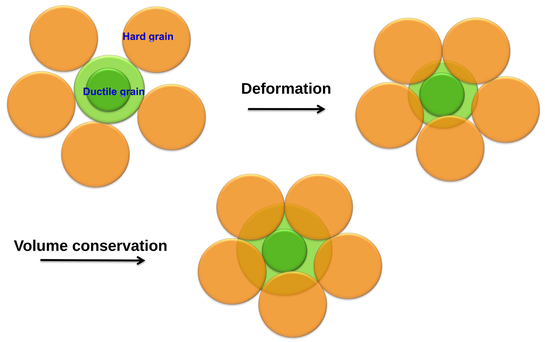

Fig. 2(b). Soft-shell model sphere; grains can interpenetrate until their inner rigid cores come into contact. The radius of the rigid core is a good proxy for ductility of the grains (*Mousavi & Bryant 2007*). This is a schematic of pressing one ductile grain into five hard grains. The overlap stops when the hard grain reaches the rigid core of ductile grain. Volume conservation is calculated at the end and added to the outer shell of ductile grain. The ductile grain fills the pore space between grains similar to squishing of ductile grain into pore space between grains, in Fig. 2(a).

Fig. 3(a). Overgrowth quartz cementation (*Image courtesy of Kitty Milliken, BEG*).

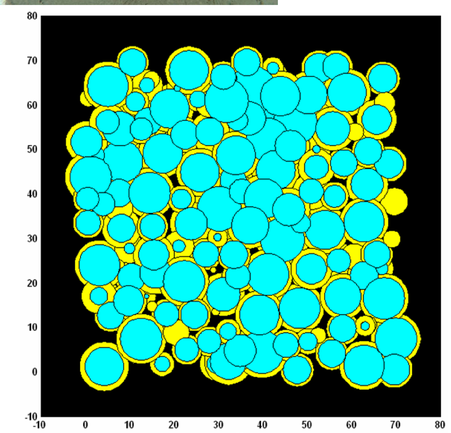

Fig. 3(b). A 2D thin section of a dense random packing of 1000 spheres in a bi-dispersed packing (radius ratio of 1.5 and 50% small spheres) with 30% ductile spheres (with 0.7 rigid radius). We grew 20% overgrowth cement (0.2 of the sphere radius) on the grains and reduced the porosity to 7%. The original porosity in this packing was 22%.

Network Modeling

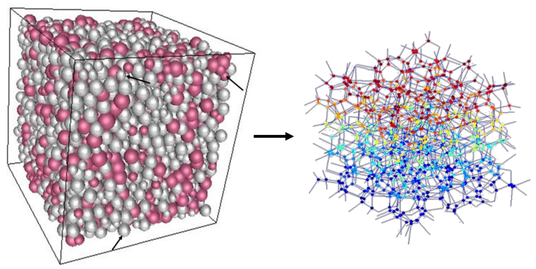

Fig. 4(a). From the model sandstone (left) we extract a network model of pore space (right), which is an easy and effective tool for determining flow properties of the model rock. The network model represents pore space as a graph of interconnected sites. The nodes of the graph represent pore bodies, while the lines connecting nodes indicate the pore throats which connect pore bodies to flow.

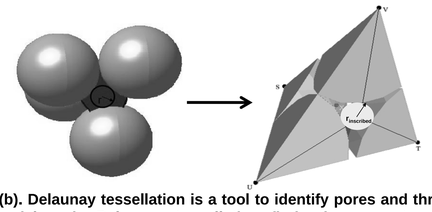

Fig. 4(b). Delaunay tessellation is a tool to identify pores and throats in the model rock. Delaunay tessellation finds the nearest neighbor spheres in the packing and groups them in tetrahedral. A pore body is the empty space between four spheres in tetrahedron, and a pore throat is empty space between three spheres of each face. These data will be used to build a network model.

Connectivity of Pore Space: Effect of Epitaxial Cement

Average connectivity of the pore space is the number of the open throats in each pore in the packing. For a packing of spheres with all of the throats open, the connectivity is 4 because each pore in Delaunay cell has four open throats. We have computed the average connectivity of pore space during simulated cementation and ductile deformation in tight gas sandstones. Both of these processes will close some of the pore space and related pore throats in those rocks. Therefore the average connectivity of those packing should be below 4.

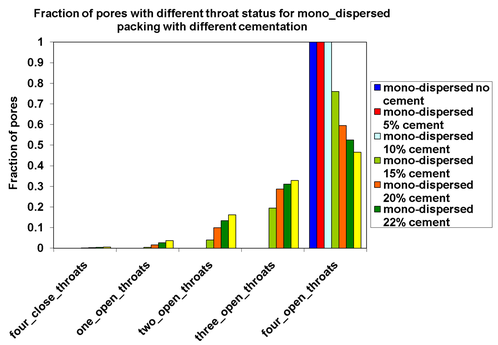

Fig. 5(a). Fraction of pores with different throat status for mono dispersed packing with different cementation. By increasing cement we reduce the amount of open throats and increase the throats closure.

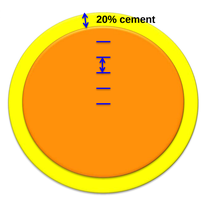

Fig. 5(b). 20% cement for example means the 20% of the size of the grain radius will be added to the outer surface of the grain.

Connectivity of Pore Space: Effect of Epitaxial Cement (cont.)

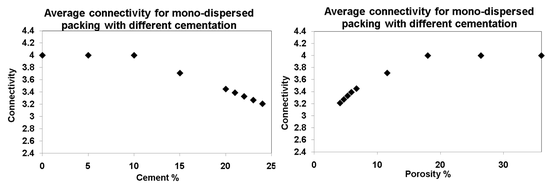

Fig. 6. Average connectivity of pore space for a mono-dispersed packing with different amount of cement (left). By increasing the amount of cement, the connectivity of pore space reduces because the fraction of pores containing blocked throats, increases (previous figure). The right figure is the same data with porosity in x axis. By increasing the cement, the porosity of packings also reduces.

Connectivity of Pore Space: Effect of Ductile Grain Deformation and Epitaxial Cement

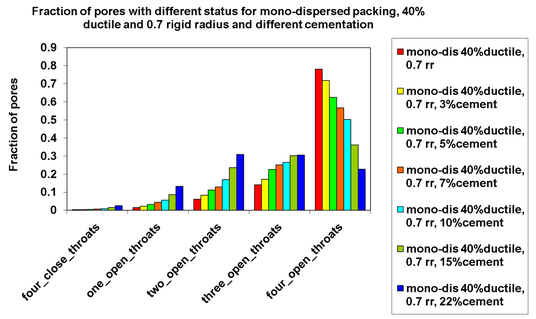

Fig. 7. Fraction of pores with different throat status for mono dispersed packing of 40% ductile 0.7 rigid radius and different cementation. By increasing cement in the original packing, we increase the fraction of pores with higher close throats.

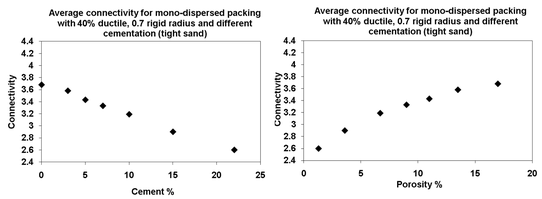

Fig. 8. Average connectivity of pore space for mono-dispersed packing with 40% ductile, 0.7 rigid radius and different amount of cement (left). The right side shows the trend with porosity reduction. By adding more cement the connectivity will be reduced.

AAPG Annual Convention & Exhibition 7-10 June 2009 Denver, Colorado

Connectivity of Pore Space: The Primary Control on Two-Phase Flow Properties of Tight-Gas Sands, AAPG 535743 (Part II)

Maryam A. Mousavi & Steven L. Bryant

Center for Petroleum and Geosystems Engineering, The University of Texas at Austin

Percolation Threshold

Percolation threshold is the critical fraction of lattice points that must be filled to create a continuous path spanning the lattice. Applied to fluids in pores, percolation implies a critical saturation of wetting or non-wetting fluid above which the fluid can flow.

Table 1. The bond-percolation threshold for different regular lattices. We use tetrahedral with connectivity (degree) of 4.

Lattice	Degree	Bond threshold
Hexagonal	3	0.65
Square	4	0.5
Tetrahedral	4	0.39
Triangular	6	0.347
Simple cubic	6	0.257
Face-centered cubic	12	0.125
Voronoi	16.27	0.0822

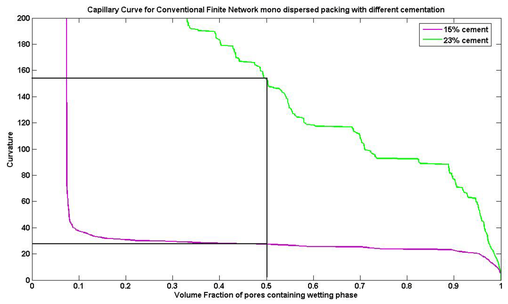

Fig. 9. To calculate the bond percolation threshold we used the curvature (capillary pressure) at 50% wetting phase saturation. This figure shows the drainage simulation for mono dispersed packing with 15 (porosity = 12) and 23% cement (porosity = 4.7%). The line shows the 50% saturation of wetting phase for both packings. For packing with higher amount of cement or lower porosity, the capillary pressure shows higher value. This is related to lower connectivity (smaller throats and lots of blocked throats) in lower porosity packing.

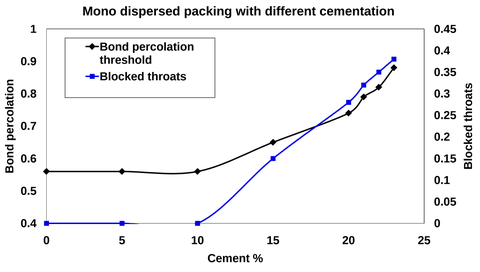

Fig. 10(a). Gas phase in the model rocks was assumed to percolate in the pore space during drainage at 50% wetting phase saturation. By adding cement to mono-dispersed packing, we reduce the porosity, increase the number of blocked throats and therefore increase the bond percolation threshold. This is a mono dispersed packing with different amount of cementation.

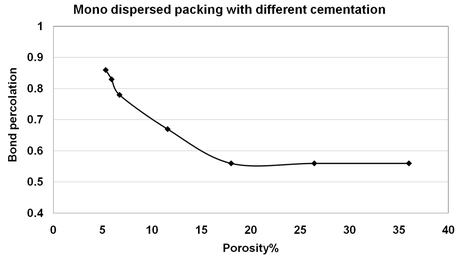

Fig. 10(b). The same data plotted against porosity. By increasing the bond percolation threshold (increasing cement), the porosity reduces.

Percolation Threshold (cont.)

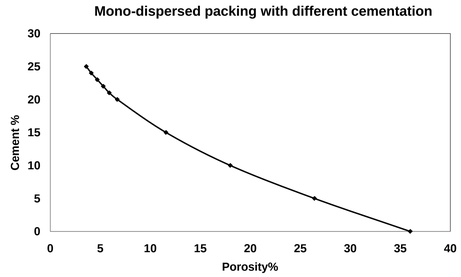

Fig. 10(c). Cement versus porosity for selected packings from Fig. 10a. Heavily cemented packings have small porosity, high percolation threshold and high blocked throats.

Bond Percolation Threshold for Tight Gas Sand Model

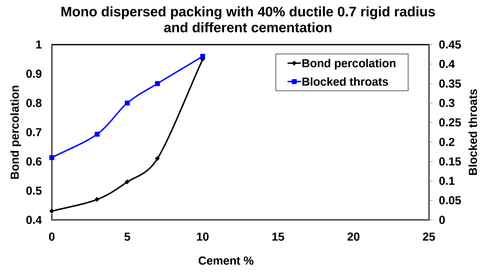

Fig. 11(a). Increasing cement in a packing with 40% ductile matter and 0.7 rigid radius of soft grains causes the percolation threshold to increase, because of closure of some pores and related throats resulting from cementation and ductile grain compaction. By comparing this plot with Fig. 9, it is clear that with small portion of cement here, we have higher blocked throats and consequently higher bond percolation threshold. This is related to compaction of ductile grains which make the throats smaller. (look at pore throat size distribution on Fig. 15b).

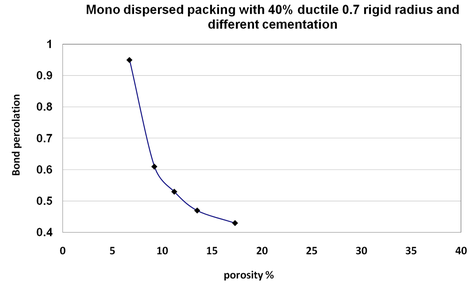

Fig. 11(b). The same packings with percolation versus porosity. Packings with higher bond percolation threshold have smaller porosities. By comparing this plot with Fig. 9b, we realize that bond percolation is not a function of porosity because packings with almost the same porosity have different bond percolation threshold.

Bond Percolation Threshold for Tight Gas Sand Model (cont.)

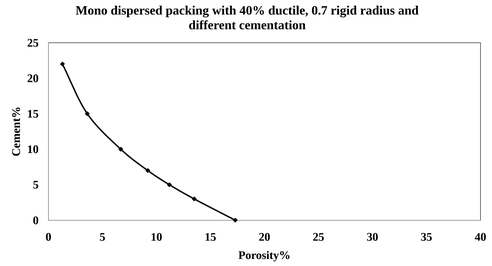

Fig. 11(c). Cement versus porosity for selected packings from Fig. 11a. By comparing this plot with Figs. 11a and 11b we can see that in the case of heavily cemented packings (15% and 22% cement), the gas phase didn't percolate at 50% wetting phase which is related to highly blocked throats for those packings.

IMPLICATION: The larger percolation threshold in low-porosity sandstone means larger gas phase saturations are required to maintain connectivity of the gas phase. Conversely, small increments in water saturation will reduce gas connectivity and therefore reduce gas effective permeability.

Drainage Simulation

Drainage was calculated using network model. We use critical curvature of the throats to quantify the network model in drainage simulation. This critical curvature is a value that assigns to throats based on their inscribed radius and is the minimum curvature for non-wetting phase to pass through a throat with wetting phase. To calculate this curvature we used the Hainse criteria (insphere approximation) (Haines 1930) with Mason and Mellor 1995 modification because meniscus between non-wetting and wetting phases in this method is considered to be sphere. Mason and Mellor subtract 1.6 from Haines criteria to come up with overestimation of critical curvature. We used the equation below to calculate the critical curvature:

$$C = 2R_{mean} / R_{inscribed} - 1.6$$

Where R_{mean} is the mean radius of packing and $R_{inscribed}$ is the radius of inscribed sphere between three spheres in each face of Delaunay cell (Fig. 4b).

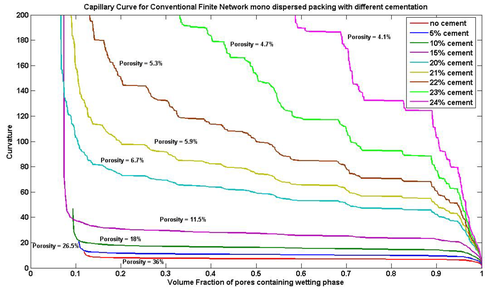

Fig. 12(a). Drainage simulation for mono-dispersed packing with different cementation. By increasing the amount of cement, the capillary pressure and irreducible water saturation of the packing increase. The shape of the drainage curve for low porosities changes because the pore space is poorly connected in highly cemented packings.

Drainage Simulation (cont.)

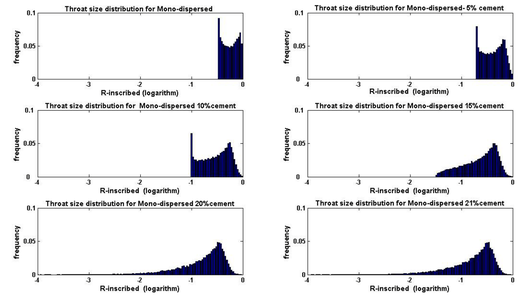

Fig. 12(b). Throat size distribution ($R_{inscribed}$, Logarithm values) for selected packings from Fig. 12a. By increasing amount of cement the throats distribution changes to wider shape and smaller throats. The frequency of blocked throats (inscribed radius less than 1e-12) are not shown.

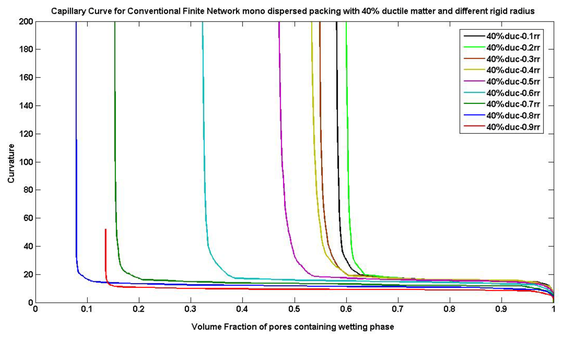

Fig. 13(a). Drainage simulation for mono-dispersed packing with 40% ductile matter and different rigid radius. By decreasing the rigid radius of ductile grains (increasing the ductility of soft grains) the irreducible water saturation increases.

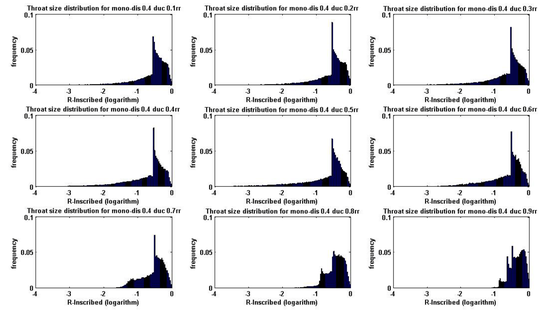

Fig. 13(b). Throat size distribution ($R_{inscribed}$, Logarithm values) for selected packings from Fig. 13a. By decreasing the rigid radius (increasing ductility of soft grains) the throats distribution changes to wider shape and smaller throats. The drainage curves are different than when we only have cement which is related to different shape of throat size histogram. The frequency of blocked throats is not shown in this picture.

AAPG Annual Convention & Exhibition 7-10 June 2009 Denver, Colorado

Connectivity of Pore Space: The Primary Control on Two-Phase Flow Properties of Tight-Gas Sands, AAPG 535743 (Part III)

Maryam A. Mousavi & Steven L. Bryant

Center for Petroleum and Geosystems Engineering, The University of Texas at Austin

Drainage Simulation (cont.)

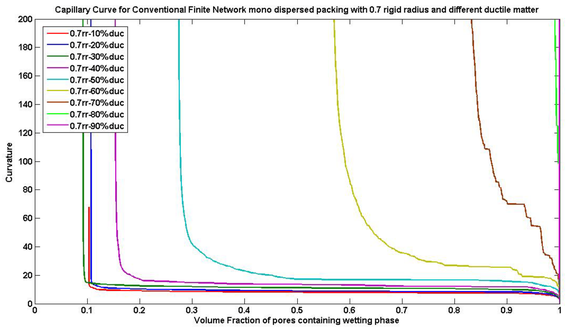

Fig. 14(a). Drainage simulation for mono-dispersed packing with 0.7 rigid radius and different ductile matter. By increasing the amount of ductile grains in the packing, the irreducible water saturation increases more rapidly than when we change the rigid radius only.

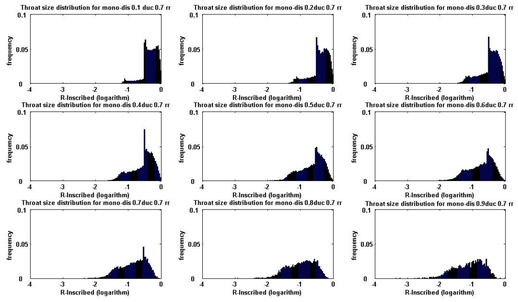

Fig. 14(b). Throat size distribution ($R_{inscribed}$, Logarithm values) for selected packings from Fig. 14a. By increasing the amount of ductile grains in packing, the throats distribution changes to wider shape and smaller throats. The frequency of blocked throats is not shown in this picture.

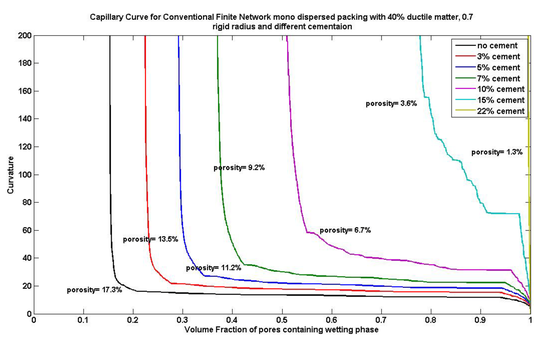

Fig. 15(a). Drainage simulation for mono-dispersed packing with 40% ductile matter, 0.7 rigid radius and different cementation. By increasing the amount of cement in these packings (tight sands) the capillary pressure and irreducible water saturation increase.

Drainage Simulation (cont.)

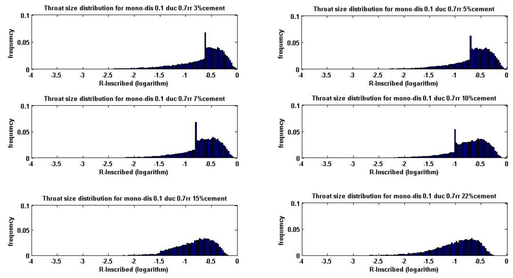

Fig. 15(b). Throat size distribution ($R_{inscribed}$, Logarithm values) for selected packings from Fig. 15a. By increasing amount of cement, the throats distribution changes to wider shape and smaller throats. The frequency of blocked throats is not shown in this picture.

Effective Medium Theory: Permeability Estimation

We can estimate absolute permeability of a network using effective medium theory. We can then estimate gas phase relative permeability by computing the effective conductivity of the portion of the network occupied by gas phase. The effective conductivity g_m satisfies the following equation:

$$\int \frac{g_m - g}{g_m\left(\frac{z}{2}-1\right)+g} f(g)dg = 0$$

Where:
g_m = effective conductivity,
g = values of bond conductance,
z = connectivity of lattice, which is 4 in our case (using tetrahedron)
f(g)dg = frequency distribution of bond conductance

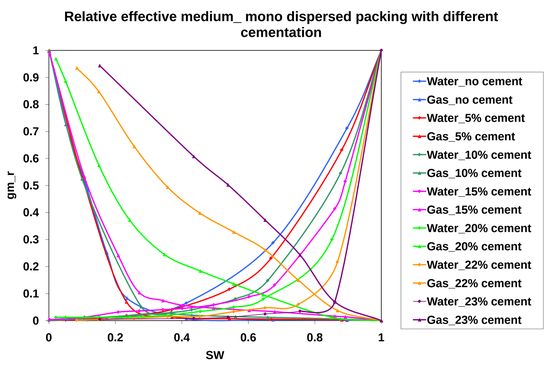

Fig. 16. Drainage relative permeability (effective medium) for mono dispersed packing with different cementation. By increasing the cement, the connectivity of pore space decreases and the water perm shifts toward right because throats containing water become smaller by increasing cement. The gas perm shows higher relative values as cement increases. This is a consequence of the connectivity of pore space.
In the case of low porosity packings, the fraction of the drained throats are bigger at 50% volume fraction of wetting phase (saturation) compare to higher porosity packings. Packings with lower porosity are poorly connected and a larger fraction of throats needs to be drained too get the same volume fraction of wetting phase (50% saturation) compare to packings with higher porosity, Fig. 17.

Effective Medium Theory: Permeability Estimation (cont.)

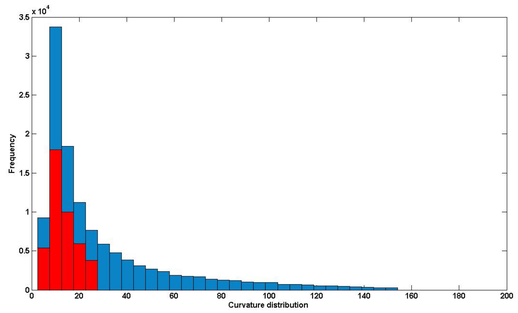

Fig. 17(a). Curvature (capillary pressure) distribution for mono-dispersed packing with 15% cement (porosity = 12%). The blue color shows distribution for all throats; the red color shows the distribution of throats drained when the wetting phase saturation is 50% and the gas phase is assumed to reach percolation threshold. The drained throats amount to 35% of the total throats in the packing including blocked throats.

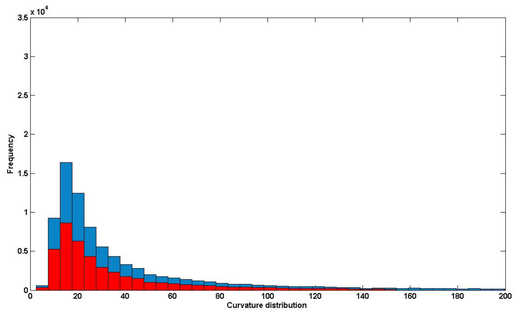

Fig. 17(b). Curvature (capillary pressure) distribution for mono-dispersed packing with 23% cement (porosity = 4.7%). The blue color shows distribution for all throats; the red color shows the distribution of throats drained when the wetting phase saturation is 50% and the gas phase is assumed to reach percolation threshold. The drained throats are 47% of the total throats in the packing including blocked throat. This is larger fraction than for the higher porosity packing in Fig. 17a. This explains why the gas phase relative permeability is larger in the low porosity packing, Fig. 16. The fraction of big throats (lower curvature values) are smaller in this case compare to Fig. 17a which implies smaller throat sizes. The high values of curvature (small and blocked throats) are not shown in this figure.

Key Finding

Connectivity of the matrix pore space is a critical factor for understanding flow properties of tight gas sandstones.

Conclusions

Grain scale simulation of porosity-reducing mechanisms in tight gas sandstones (ductile grain deformation, cement precipitation) shows that pore space is poorly connected in these rocks. The connectivity decreases rapidly as porosity decreases, once the porosity is less than 10%. The poor connectivity makes drainage curves highly sensitive to small changes in porosity.

In addition to reducing connectivity, the porosity-reducing mechanisms change pore throat size distributions in a nonlinear fashion. This affects the phase relative permeabilities. Simulation of drainage in model tight gas sands shows that the water relative permeability curve shifts toward smaller values and gas relative permeability shifts toward higher values.

References

Haines, W. B. (1930). "Studies in the Physical Properties of Soil. V. The Hysteresis Effects in Capillary Properties and the Modes of Moisture Distribution Associated Therewith," Journal of Agricultural Sciences 20: 97.

Mason G., and Mellor D. W. (1995). "Simulation of Drainage and Imbibitions in a Random Packing of Equal Spheres," Journal of Colloid and Interface Science 176: 214-225.

Mousavi, M.A., Bryant, S.L., (2007). "Geometric Models of Porosity Reduction Mechanisms in Tight Gas Sands," Paper presented at Rocky Mountain Oil & Gas Technology Symposium, Denver, Colorado, April.